

Selective $^{226}\text{Ra}^{2+}$ Ionophores Provided by Self-Assembly of Guanosine and Isoguanosine Derivatives

Fijs W. B. van Leeuwen,[†] Willem Verboom,^{*,†} Xiaodong Shi,[‡] Jeffery T. Davis,[‡] and David N. Reinhoudt^{*,†}

Contribution from the Laboratory of Supramolecular Chemistry and Technology, Mesa⁺ Research Institute, University of Twente, P.O. Box 217, 7500 AE Enschede, The Netherlands, and Department of Chemistry and Biochemistry, University of Maryland, College Park, Maryland 20742

Received July 23, 2004; E-mail: w.verboom@utwente.nl

Abstract: The self-assembled guanosine (G **1**)-based hexadecamers and isoguanosine (isoG **2**)-based decamers are excellent $^{226}\text{Ra}^{2+}$ selective ionophores even in the presence of excess alkali (Na^+ , K^+ , Rb^+ , and Cs^+) and alkaline earth (Mg^{2+} , Ca^{2+} , Sr^{2+} , and Ba^{2+}) cations over the pH range 3–11. G **1** requires additional picrate anions to provide a neutral assembly, whereas the isoG **2** assembly extracts $^{226}\text{Ra}^{2+}$ cations without any such additives. Both G **1**–picrate and isoG **2** assemblies show $^{226}\text{Ra}^{2+}$ extraction even at a 0.35×10^6 fold excess of Na^+ , K^+ , Rb^+ , Cs^+ , Mg^{2+} , or Ca^{2+} (10^{-2} M) to $^{226}\text{Ra}^{2+}$ (2.9×10^{-8} M) and at a 100-fold salt to ionophore excess. In the case of the G **1**–picrate assembly, more competition was observed from Sr^{2+} and Ba^{2+} , as extraction of $^{226}\text{Ra}^{2+}$ ceased at an $\text{M}^{2+}/^{226}\text{Ra}^{2+}$ ratio of 10^6 and 10^4 , respectively. With the isoG **2** assembly, $^{226}\text{Ra}^{2+}$ extraction also occurred at a $\text{Sr}^{2+}/^{226}\text{Ra}^{2+}$ ratio of 10^6 but ceased at a 10^6 excess of Ba^{2+} . The results clearly demonstrate the power of molecular self-assembly for the construction of highly selective ionophores.

Introduction

Inhalation or ingestion of Ra^{2+} , a notorious bone seeker, can cause cancer and severe developmental or immunological problems. The toxicity of $^{226}\text{Ra}^{2+}$ is not solely due to its gamma and alpha particle emission, as the daughter nuclides, radon-222, polonium-218, and lead-214, also contribute to in vivo radiotoxicity.¹ As a naturally occurring radioactive material (NORM),² Ra^{2+} is a subsurface pollutant in, e.g., ores, oil and gas, and drinking water. In the industries utilizing these subsurface products, Ra^{2+} salts precipitate in production pipes as scales and sludges, while the nonprecipitated Ra^{2+} cations are released into the environment with the “produced water”. The resulting “technologically enhanced NORM” (TENORM)³ wastes increase this radionuclide’s health risks.

The TENORM waste contains a large excess of alkali and alkaline earth cations relative to Ra^{2+} .⁴ Therefore, Ra^{2+} separation from more abundant cations requires selective methods. Precipitation,⁵ absorption,^{6–8} and extraction^{9–12} techniques have

all been used for the selective removal and/or detection of Ra^{2+} . The few Ra^{2+} extraction procedures use crown-ether-like compounds with ionizable groups that allow for overall neutrality of the resulting salt–crown complex. The synergistic cation extraction by a crown ether and a lipophilic carboxylate pair,¹⁰ or extraction using crown ethers that are functionalized with acidic side chains,^{11,12} render anion coextraction unnecessary. However, the drawbacks to these crown ethers as extractants include the considerable effort often required for their synthesis and the limitation that they function only over a limited pH range,¹¹ since cation extraction depends on the ionization state of the acidic groups.

Nature uses molecular self-assembly to form many receptors and would also provide a powerful tool for the formation of selective ionophores.¹³ Guanosine-rich nucleic acids are well-known to coordinate alkali and alkaline earth cations using the G-quartet motif.^{14,15} Synthetic guanosine derivatives also form highly organized and well characterized structures in the presence of a range of monovalent and divalent cations.¹⁶ As

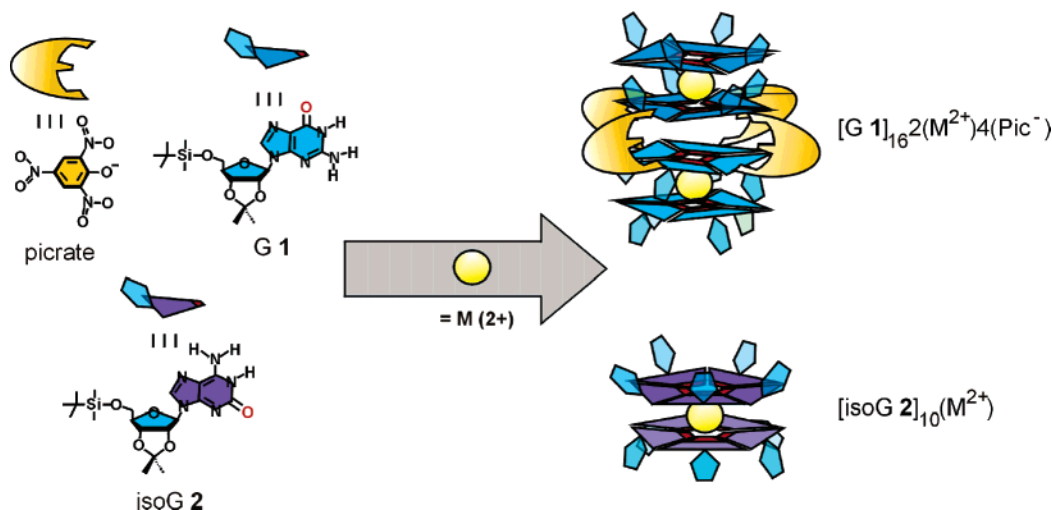
[†] University of Twente.

[‡] University of Maryland.

- (1) Toxicological Profile for Radium. *Agency for Toxic Substances and Disease Registry*; U.S. Public Health Service in collaboration with U.S. Environmental Protection Agency: 1990.
- (2) Eisenbud, M.; Gesell, T. F. *Environmental Radioactivity – From Natural, Industrial, and Military Sources*, 4th ed.; Academic Press: New York, 1997.
- (3) Cohen, S. et al. *Diffuse NORM Wastes – Waste Characterization and Preliminary Risk Assessment*. U. S. Environmental Protection Agency Office of Radiation and Indoor Air: Washington, D. C., 1993.
- (4) Wiegand, J.; Feige, S. *Origin of Radium in High-Mineralized Waters*; IAEA: Vienna, 2002.
- (5) Curie, M. S. *Century Magazine* **1904**, 461–466.
- (6) Moon, D. S.; Burnett, W. C.; Nour, S.; Horwitz, E. P.; Bond, A. *Appl. Radiat. Isot.* **2003**, 59, 255–262.

- (7) Purkl, S.; Eisenhauer, A. *J. Radioanal. Nucl. Chem.* **2003**, 256, 473–480.
- (8) Komarneni, S.; Kozai, N.; Paulus, W. *J. Nature* **2001**, 410, 771.
- (9) McDowell, W. J.; Arndsten, B. A.; Case, G. N. *Solvent Extr. Ion Exch.* **1989**, 7, 377–393.
- (10) Dietz, M. L.; Chiarizia, R.; Horwitz, E. P. *Anal. Chem.* **1997**, 69, 3028–3037.
- (11) Chen, X. Y.; Ji, M.; Fisher, D. R.; Wai, C. M. *Inorg. Chem.* **1999**, 38, 5449–5452.
- (12) Beklemishev, M. K.; Elshani, S.; Wai, C. M. *Anal. Chem.* **1994**, 66, 3521–3527.
- (13) Whitesides, G. M.; Grzybowski, B. *Science* **2002**, 295, 2418–2421.
- (14) Laughlan, G.; Murchie, A. I. H.; Norman, D. G.; Moore, M. H.; Moody, P. C. E.; Lilley, D. M. J.; Luisi, B. *Science* **1994**, 265, 520–524.
- (15) Deng, J.; Xiong, Y.; Sundaralingam, M. *PNAS* **2001**, 98, 13665–13670.

Scheme 1. Cation Induced Self-Assembly of Guanosine (G 1) Giving an 8:1 Ionophore–Cation Stoichiometry and Isoguanosine (isoG 2) Giving a 10:1 Stoichiometry^a



^a These stoichiometries are based on their Ba²⁺ and Cs⁺ complexes, respectively.^{18,19}

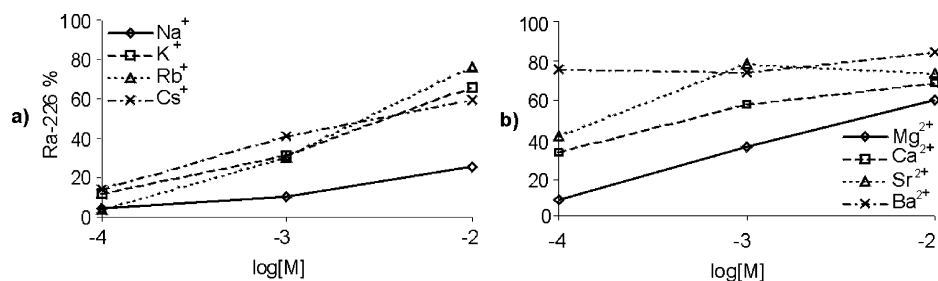


Figure 1. ²²⁶Ra²⁺ (%) present in aqueous solutions with varying concentrations of alkali(ne earth) cations at blank conditions. Different salt concentrations Mⁿ(NO₃)_n [(a) M = Na⁺, K⁺, Rb⁺, and Cs⁺; (b) M = Mg²⁺, Ca²⁺, Sr²⁺, and Ba²⁺] and fixed ²²⁶Ra²⁺ (2.9 × 10⁻⁸ M) concentrations were used.

schematically depicted in Scheme 1, X-ray crystallography has shown that the guanosine (G 1) derivative forms noncovalent assemblies that are based on (G 1)₈–M⁽⁺⁾ octamers, while the isoguanosine (isoG 2) derivative forms decamers in the presence of a templating cation. The G 1 assembly has a relatively high K⁺, Sr²⁺, and Ba²⁺ affinity,^{17,18} whereas the isoG 2 assembly shows strongest affinity for the larger Cs⁺ and Ba²⁺ cations.^{19,20} This cation binding selectivity is attributed to the geometry of the hydrogen bond donors and acceptors: G 1 forms tetramers, whereas isoG 2 prefers to form hydrogen-bonded pentamers in the presence of the cation template. In addition, recent calculations on a series of (isoG)_n–M⁺ complexes support our experimental observations that (isoG)₅–M⁺ pentamers are favored over the (isoG)₄–M⁺ tetramers by the alkali metal cations larger than Li⁺.²¹ The macrocycle cavity size of these self-assembled ionophores determines the cation binding selectivity.

Our goal is to develop Ra²⁺-selective ionophores. In separations of Group I and II cations, selectivity is often controlled by the ionophore cavity size. A self-assembled receptor with multiple oxygen donors and a cavity that fits the Ra²⁺ coordination sphere is a logical start for identifying Ra²⁺ ionophores. Since G 1–picrate and isoG 2 assemblies were shown to possess high affinities for cations similar to Ra²⁺, we reasoned they might be excellent candidates for Ra²⁺ coordination.

Here, we report on the extremely high ²²⁶Ra²⁺ extraction selectivity of assemblies formed by the lipophilic nucleosides G 1 and isoG 2, even in the presence of alkali and alkaline earth cations and over a wide pH range.

Results and Discussion

Precipitation of ²²⁶Ra²⁺. During blank ²²⁶Ra²⁺ extraction experiments performed in the presence of varying concentrations of alkali and alkaline earth metal nitrates, a deficit in detected ²²⁶Ra²⁺ cations, as compared to the actual amount added, was observed. Experiments showed a decrease of ²²⁶Ra²⁺ cations in the aqueous phase (Figure 1); however, ²²⁶Ra²⁺ cations could not be detected in the organic phase. This suggests that under these extraction conditions ²²⁶Ra²⁺ salts precipitate on the glass wall of the vials used, which would be a form of “scale/sludge formation” similar to that causing contamination of production pipes in industry.² To obtain insight into the influence of the different competing cations and their abundance on this “precipitation” of ²²⁶Ra²⁺ salts, the deficiency starting from the same ²²⁶Ra²⁺ concentration (2.9 × 10⁻⁸ M) was monitored in

- (16) Davis, J. T. *Angew. Chem., Int. Ed.* **2004**, *43*, 668–698.
 (17) Forman, S. L.; Fettingner, J. C.; Pieraccini, S.; Gottarelli, G.; Davis, J. T. *J. Am. Chem. Soc.* **2000**, *122*, 4060–4067.
 (18) Shi, X. D.; Mullaugh, K. M.; Fettingner, J. C.; Jiang, Y.; Hofstadler, S. A.; Davis, J. T. *J. Am. Chem. Soc.* **2003**, *125*, 10830–10841.
 (19) (a) Cai, M. M.; Marlow, A. L.; Fettingner, J. C.; Fabris, D.; Haverlock, T. J.; Moyer, B. A.; Davis, J. T. *Angew. Chem., Int. Ed.* **2000**, *39*, 1283–1288. (b) Shi, X.; Fettingner, J. C.; Cai, M. M.; Davis, J. T. *Angew. Chem., Int. Ed.* **2000**, *39*, 3124–3127.
 (20) Lee, S. C.; Lamb, J. D.; Cai, M. M.; Davis, J. T. *J. Inclusion Phenom.* **2001**, *40*, 51–57. The ²²⁶Ra²⁺ selectivity of the isoG 2 assembly is in agreement with competitive liquid membrane experiments, showing that the isoG 2 assembly transports Ba²⁺ nitrate across supported liquid membranes much faster than it does the corresponding Na⁺ and K⁺ nitrate salts.
 (21) Meyer, M.; Suhnel, J. *J. Phys. Chem. A* **2003**, *107*, 1025–1031.

the presence of varying concentrations of different salts ($M = \text{Na}^+, \text{K}^+, \text{Rb}^+, \text{Cs}^+, \text{Mg}^{2+}, \text{Ca}^{2+}, \text{Sr}^{2+}, \text{and } \text{Ba}^{2+}$).

Monovalent alkali cations (Figure 1a) gave rise to large deficiencies of $^{226}\text{Ra}^{2+}$ cations in solutions with low concentrations of alkali cations ($< 10^{-3}$ M). In particular, the presence of the smallest and hardest cation (Na^+) caused a significant deficiency of $^{226}\text{Ra}^{2+}$ cations, even at 10^{-2} M. The other cations ($\text{K}^+, \text{Rb}^+, \text{and } \text{Cs}^+$) gave smaller deficiencies at concentrations of 10^{-2} M and a highly similar $^{226}\text{Ra}^{2+}$ “precipitation” behavior.

In the case of the alkaline earth cations (Figure 1b), deficiencies of detected $^{226}\text{Ra}^{2+}$ cations were significantly lower than those observed with the alkali cations. This may be a result of the similar chemistry of the alkaline earth cations, including $^{226}\text{Ra}^{2+}$. As a result Ba^{2+} , the cation most similar to $^{226}\text{Ra}^{2+}$, caused the smallest deficiency of $^{226}\text{Ra}^{2+}$ cations. Nevertheless, the smaller and harder alkaline earth cations, viz. $\text{Mg}^{2+}, \text{Ca}^{2+}$, and to a lesser extent Sr^{2+} , showed significant “precipitation” of $^{226}\text{Ra}^{2+}$ at the lower salt concentrations (Figure 1b ($\log[M] < -2$)). At salt concentrations of 10^{-2} M the “precipitation” of $^{226}\text{Ra}^{2+}$ salts significantly decreased in all cases.

The “deficiency” data (Figure 1) suggest that, in extraction experiments (vide infra), the actual amount of $^{226}\text{Ra}^{2+}$ cations present in solution can be somewhat lower than the amount (2.9×10^{-8} M) of $^{226}\text{Ra}^{2+}$ cations added. However, we have found that the assemblies formed by the nucleosides **G 1** and **isoG 2** not only provide excellent $^{226}\text{Ra}^{2+}$ selective ionophores but also for the greater part reduce the amount of $^{226}\text{Ra}^{2+}$ salt precipitates.

Noncompetitive $^{226}\text{Ra}^{2+}$ Extraction Experiments. To evaluate the $^{226}\text{Ra}^{2+}$ extraction ability of **G 1** and **isoG 2** assemblies, liquid–liquid extractions were first performed under noncompetitive conditions. In each experiment, the aqueous phase contained the same concentration of added $^{226}\text{Ra}^{2+}$ cations ($^{226}\text{Ra}_{\text{add}}^{2+} = 2.9 \times 10^{-8}$ M) and the organic phase contained 10^{-4} M of self-assembled ionophore, assuming complete formation of the (**G 1**)₈- M^{2+} and the (**isoG 2**)₁₀- M^{2+} complexes. The **G 1** assembly only extracted $^{226}\text{Ra}^{2+}$ cations when picrate anions were present in the aqueous phase (100% extraction). In marked contrast, the **isoG 2** assembly extracted 100% of the $^{226}\text{Ra}^{2+}$ cations, both with and without picrate anions in the aqueous phase. These extraction results are consistent with previous findings that additional “stabilizing” picrate anions are needed for the formation of neutral G-quadruplex structures using **G 1**,^{17,18} whereas cation-templated formation of the **isoG 2** decamer is known to be anion independent.^{19,20}

Binding Potential of **G 1–Picrate and **isoG 2** Assemblies for Divalent Alkaline Earth Cations.** To study whether **G 1**–picrate and **isoG 2** assemblies have a binding affinity for alkaline earth cations ($\text{Mg}^{2+}, \text{Ca}^{2+}, \text{Sr}^{2+}, \text{and } \text{Ba}^{2+}$), the relative extraction ability of **G 1**–picrate and **isoG 2** assemblies under noncompetitive conditions, using nonradioactive nitrate salts (10^{-4} M), were determined with inductively coupled plasma mass spectrometry (ICP-MS). The results are summarized in Table 1.

The **G 1**–picrate assembly shows high relative extraction abilities for Sr^{2+} and Ba^{2+} , compared to Ca^{2+} and Mg^{2+} cations. In the case of the **isoG 2** assembly in general a lower extraction ability is observed, which may be due to the lack of a lipophilic anion such as picrate to facilitate partitioning of metal ions into the organic phase. However, the **isoG 2** assembly still allows

Table 1. Extraction Percentages of $\text{Mg}^{2+}, \text{Ca}^{2+}, \text{Sr}^{2+}, \text{and } \text{Ba}^{2+}$ Cations by **G 1**–Picrate and **isoG 2** Assemblies, at an Equimolar Self-Assembled Ionophore to Cation Concentration (10^{-4} M), Determined by ICP-MS^a

ionophore	Mg^{2+} (%)	Ca^{2+} (%)	Sr^{2+} (%)	Ba^{2+} (%)
G 1 –picrate	2	39	90	84
isoG 2	1	57	32	48

^a In all cases metal nitrate salts were used. ^b Extraction percentages were verified under identical conditions with a ^{133}Ba tracer.

about 50% extraction of Ca^{2+} and Ba^{2+} cations under these conditions.

Competitive $^{226}\text{Ra}^{2+}$ Extraction Experiments in the Presence of Alkaline Earth Cations. To determine whether $^{226}\text{Ra}^{2+}$ would be extracted in competition with $\text{Mg}^{2+}, \text{Ca}^{2+}, \text{Sr}^{2+}, \text{and } \text{Ba}^{2+}$, extractions were performed under the same conditions as those used for the ICP-MS analyzed extractions (Table 1). For these $^{226}\text{Ra}^{2+}$ extraction experiments, a ratio of $^{226}\text{Ra}^{2+}$ cations to competing alkaline earth cations of 2.9×10^{-8} M to 10^{-4} M was used.

After adding $^{226}\text{Ra}^{2+}$ cations, competitive extraction experiments with **G 1**–picrate and **isoG 2** assemblies revealed high $^{226}\text{Ra}^{2+}$ selectivities with all four competing cations. This means that both nucleosides are able to selectively extract $^{226}\text{Ra}^{2+}$ from a 3.5×10^3 -fold excess of $\text{Mg}^{2+}, \text{Ca}^{2+}, \text{Sr}^{2+}, \text{and } \text{Ba}^{2+}$ cations (Figure 2; $\log([M^{2+}]/[I]) = 0$).

To determine the range in which **G 1**–picrate and **isoG 2** assemblies are effective $^{226}\text{Ra}^{2+}$ ionophores, competition experiments with the single cations ($\text{Mg}^{2+}, \text{Ca}^{2+}, \text{Sr}^{2+}, \text{and } \text{Ba}^{2+}$) were carried out. The smallest of the alkaline earth cations Mg^{2+} showed high $^{226}\text{Ra}^{2+}/\text{Mg}^{2+}$ extraction selectivities for both the **G 1**–picrate and **isoG 2** assemblies. At a 10^6 -fold excess of Mg^{2+} to $^{226}\text{Ra}^{2+}$ cations (salt to ionophore ratio of 240), 63% of the $^{226}\text{Ra}^{2+}$ cations were still extracted (Figure 2a; $\log([Mg^{2+}]/[I]) = 2.4$) by the **G 1**–picrate assembly. However, the **isoG 2** assembly (without added picrate) did not show any interference in its ^{226}Ra extraction percentage by Mg^{2+} , which is a common cation in saline waters containing Ra^{2+} .⁴ The **isoG 2** assembly can quantitatively remove $^{226}\text{Ra}^{2+}$ cations from solutions containing more than a million-fold excess of Mg^{2+} cations, and the **G 1**–picrate assembly maintains a significant $^{226}\text{Ra}^{2+}$ selectivity under identical conditions.

At a $\text{Ca}^{2+}/^{226}\text{Ra}^{2+}$ ratio of 10^6 , 45% and 25% of the $^{226}\text{Ra}^{2+}$ cations were still extracted by both the **G 1**–picrate and **isoG 2** assemblies, respectively (Figure 2b; $\log([\text{Ca}^{2+}]/[I]) = 2.4$). These comparative extraction data show that assemblies of both the lipophilic nucleosides **G 1** and **isoG 2** are able to selectively remove $^{226}\text{Ra}^{2+}$ from a million-fold excess of Ca^{2+} cations.

In the presence of Sr^{2+} cations, the **isoG 2** assembly shows a remarkable $^{226}\text{Ra}^{2+}$ cation selectivity (53%; $\text{Sr}^{2+}/^{226}\text{Ra}^{2+} = 10^6$), but the **G 1**–picrate assembly fails to extract $^{226}\text{Ra}^{2+}$ above a ratio of 10^5 (Figure 2c). This results in a more than 100-fold higher selectivity in the case of the **isoG 2** assembly, allowing for $^{226}\text{Ra}^{2+}$ extraction at a million-fold excess of competing Sr^{2+} cations.

In the case of Ba^{2+} , the cation most similar in size to Ra^{2+} ,²² the $^{226}\text{Ra}^{2+}/\text{Ba}^{2+}$ extraction selectivities are significantly lower for both ionophores (Figure 2d). Whereas the **G 1**–picrate

(22) At concentrations $> 10^{-2}$ M the total detected amount of $^{226}\text{Ra}^{2+}$ cations was almost equal to that originally added ($^{226}\text{Ra}_{\text{add}}^{2+}$), which means that there are no losses due to $^{226}\text{Ra}^{2+}$ salt precipitation.

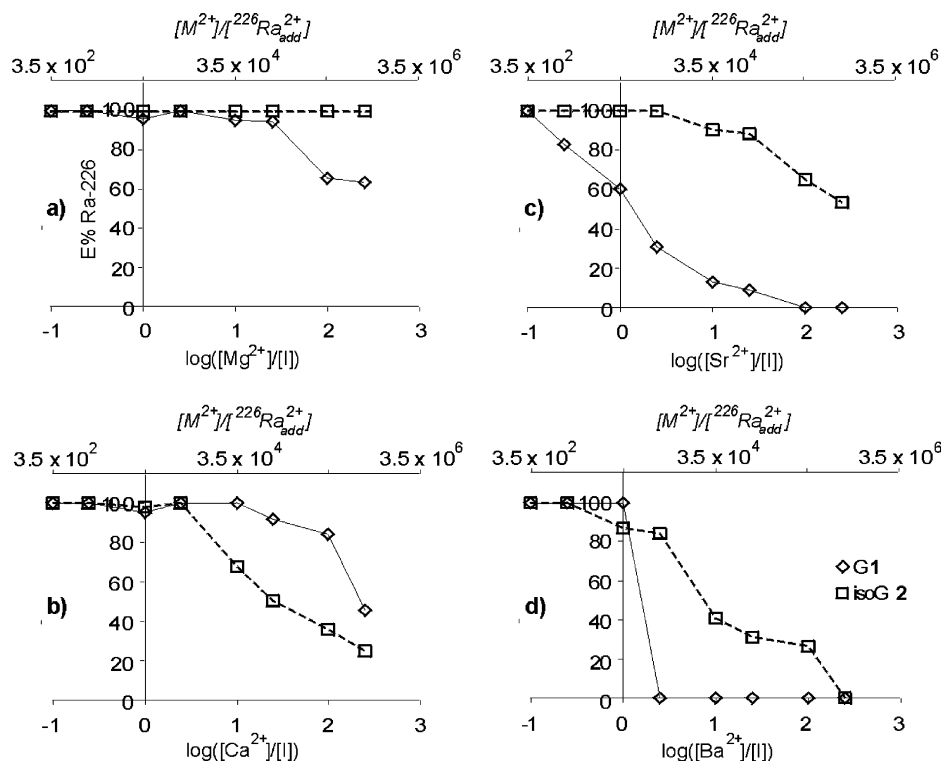
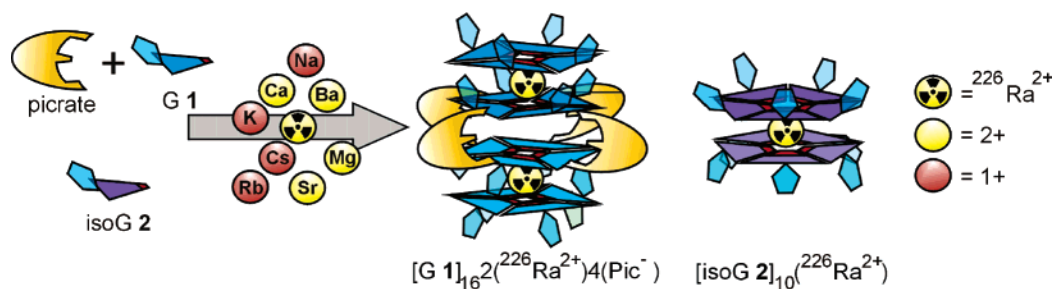


Figure 2. $^{226}\text{Ra}^{2+}$ extraction percentages recorded for different ratios of ionophore (I) to $\text{M}(\text{NO}_3)_2$ ($\text{M} = \text{Mg}^{2+}$ (a), Ca^{2+} (b), Sr^{2+} (c), or Ba^{2+} (d)), using fixed ionophore ($[(\text{G } 1)_8 + 2(\text{Pic}^-)]$ and $[(\text{isoG } 2)_{10}]$; 10^{-4} M) and $^{226}\text{Ra}^{2+}$ (2.9×10^{-8} M) concentrations. The $\log([\text{M}^{2+}]/[\text{I}])$ values correlate directly with $[\text{M}^{2+}]/[^{226}\text{Ra}_{\text{add}}^{2+}]$ values; 0 = 3.5×10^3 , 1 = 3.5×10^4 , 2 = 3.5×10^5 , and 2.4 = 0.8×10^6 .²²

Scheme 2. Selective $^{226}\text{Ra}^{2+}$ -Induced Assembly Formation of G 1 and isoG 2 in the Presence of Monovalent Alkali and Divalent Alkaline Earth Cations



assembly shows a sharp drop as soon as the Ba^{2+} concentration exceeds that of $[(\text{G } 1)_8]$ (at a $\text{Ba}^{2+}/^{226}\text{Ra}^{2+}$ ratio of 10^4 ; Figure 2d; $\log([\text{Ba}^{2+}]/[\text{I}]) = 0$), the isoG 2 assembly continues extracting $^{226}\text{Ra}^{2+}$ up to a ratio of 10^6 . The ability to differentiate between the similar chemical properties and sizes of Ba^{2+} (1.35–1.61 Å) and Ra^{2+} (1.48–1.70 Å)²³ cations suggests that the self-assembled ionophores prepared from isoG 2 are excellent $^{226}\text{Ra}^{2+}/\text{Ba}^{2+}$ selective ionophores.

In comparing the Mg^{2+} , Ca^{2+} , Sr^{2+} , Ba^{2+} , and $^{226}\text{Ra}^{2+}$ selectivities and the relative extraction ability of the G 1–picrate assembly, a trend related to the cation size can be observed. The G 1–picrate assembly has the highest affinity for Sr^{2+} and Ba^{2+} (Table 1), which is in direct agreement with previous findings that G 1-based octamers have the optimal coordination sphere for Sr^{2+} and Ba^{2+} cations.¹⁸ Therefore, the lowest $^{226}\text{Ra}^{2+}$ selectivities were observed in competition experiments with these cations (Figure 2c and d). In the case of Mg^{2+} and Ca^{2+} hardly any affinity of the G 1–picrate assembly was observed (Table 1); as a consequence, very high $^{226}\text{Ra}^{2+}$ selectivities by

the G 1–picrate assembly were obtained for these cations (Figure 2a and b). While the isoG 2 assembly shows relatively low extraction abilities for the alkaline earth cations (Table 1), it has impressive $^{226}\text{Ra}^{2+}$ selectivities in their presence (Figure 2; Scheme 2). This indicates that the isoG 2 decamer has a preference for binding the “largest” $^{226}\text{Ra}^{2+}$ (1.48–1.70 Å) cations, over the smaller alkaline earth cations (0.52–1.61 Å). This is consistent with the isoG 2 assembly being a Cs^+ (1.67–1.88 Å)²³ selective ionophore in the presence of the smaller alkali cations.²⁴

In addition to the high selectivities reported in the presence of the other alkaline earth cations, the presence of G 1 and isoG 2 in the organic phase greatly reduced the deficit of detectable $^{226}\text{Ra}^{2+}$ cations, as compared to that reported for the blank experiments (see Figure 1b). With Mg^{2+} cations the presence of G 1 and isoG 2 still allows for the detection of nearly all the $^{226}\text{Ra}^{2+}$ cations (>80%) at 10^{-4} M, which is a considerable improvement to the 10% of $^{226}\text{Ra}^{2+}$ detected under blank

(23) Shannon, R. D. *Acta Crystallogr. A* **1976**, *32*, 751–767.

(24) Davis, J. T.; Tirumala, S. K.; Marlow, A. L. *J. Am. Chem. Soc.* **1997**, *119*, 5271–5272.

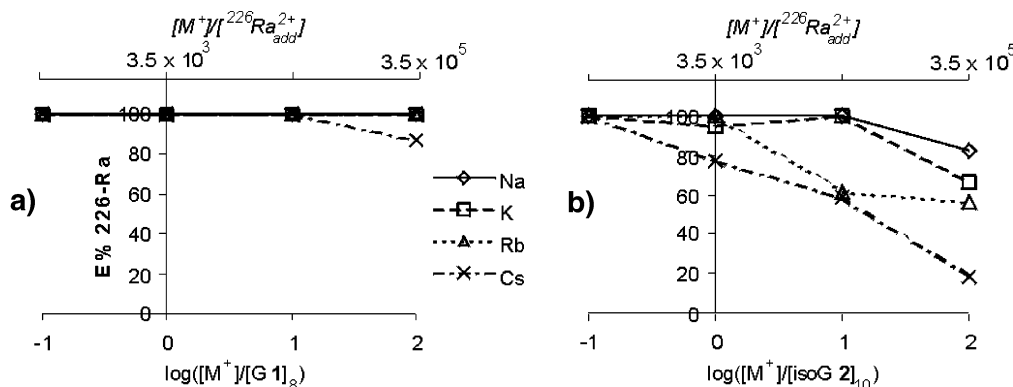


Figure 3. $^{226}\text{Ra}^{2+}$ extraction percentages recorded for different ratios of ionophore (I) to $\text{M}(\text{NO}_3)$ ($\text{M} = \text{Na}^+$, K^+ , Rb^+ , and Cs^+), using fixed ionophore ($[(\text{G } 1)_8 + 2(\text{Pic}^-)]$) (a) and $[(\text{isoG } 2)_{10}]$ (b); 10^{-4} M and $^{226}\text{Ra}^{2+}$ (2.9×10^{-8} M) concentrations. The $\log([\text{M}^+]/[\text{I}])$ values correlate directly with $[\text{M}^+]/[^{226}\text{Ra}_{\text{add}}^{2+}]$ values; $0 = 3.5 \times 10^3$, $1 = 3.5 \times 10^4$, $2 = 3.5 \times 10^5$, and $2.4 = 0.8 \times 10^6$.²⁵

conditions. IsoG 2 continues to show a near quantitative presence of $^{226}\text{Ra}^{2+}$ cations with Ca^{2+} , Sr^{2+} , and Ba^{2+} cations. In the case of G 1, the presence of Ca^{2+} and Sr^{2+} cations gave similar amounts of detected $^{226}\text{Ra}^{2+}$ cations as was reported for the blank experiments, while the presence of Ba^{2+} cations gave near quantitative amounts ($>80\%$) of detected $^{226}\text{Ra}^{2+}$ cations. These findings suggest that precipitation of $^{226}\text{Ra}^{2+}$ salts is significantly prevented by the nucleosides used. The G 1–picrate assembly and, in particular, the isoG 2 assembly not only are very selective $^{226}\text{Ra}^{2+}$ ionophores but also can prevent “ ^{226}Ra -scale formation” from solutions containing an excess of alkaline earth cations (for details see Supporting Information).

Competitive $^{226}\text{Ra}^{2+}$ Extraction Experiments in the Presence of Alkali Cations. Since Ra^{2+} -containing waters also contain relatively high concentrations of alkali cations,⁴ and previous work^{17,19} has shown that both the G 1–picrate and isoG 2 assemblies have high affinities for some of these cations, competitive extraction experiments with alkali cations were performed (Figure 3).

For both self-assembled systems of the nucleosides, G 1 and isoG 2, the $^{226}\text{Ra}^{2+}$ extraction efficiency does not seem to be perturbed by the presence of Na^+ , even at a $\text{Na}^+/\text{Ra}_{\text{add}}^{2+}$ ratio of 0.35×10^6 ; the isoG 2 assembly showed only a slight drop in $^{226}\text{Ra}^{2+}$ extraction at this point. Furthermore, both nucleosides extracted significant percentages of $^{226}\text{Ra}^{2+}$ cations in the presence of high concentrations of competing K^+ , Rb^+ , and Cs^+ cations. Figure 3 shows that impressive $^{226}\text{Ra}^{2+}$ extraction percentages were obtained for both the G 1–picrate assembly [K^+ (54%), Rb^+ (64%), Cs^+ (87%)] and the isoG 2 assembly [K^+ (66%), Rb^+ (56%), Cs^+ (18%)], even at $\text{M}^+/\text{Ra}_{\text{add}}^{2+}$ ratios of 0.35×10^6 . Since the lipophilic G 1–picrate assembly was shown to have a high K^+ affinity,¹⁷ and the isoG 2 assembly, a high Cs^+ affinity,^{20,24} it is understandable that these particular alkali cations interfere the most with $^{226}\text{Ra}^{2+}$ extraction.

In accordance with its high $^{226}\text{Ra}^{2+}$ selectivity in the presence of alkali cations, the G 1–picrate assembly shows, in all cases, near quantitative percentages of detected $^{226}\text{Ra}^{2+}$ cations, which is a significant improvement to the amounts found under blank conditions (see Figure 1a). The isoG 2 assembly, however, still shows deficiencies of $^{226}\text{Ra}^{2+}$ cations in the presence of Na^+ , K^+ , and, in particular, Cs^+ cations. As the isoG 2 assembly has its $^{226}\text{Ra}^{2+}$ extraction considerably interfered with by the presence of Cs^+ cations, the loss of $^{226}\text{Ra}^{2+}$ cations can be

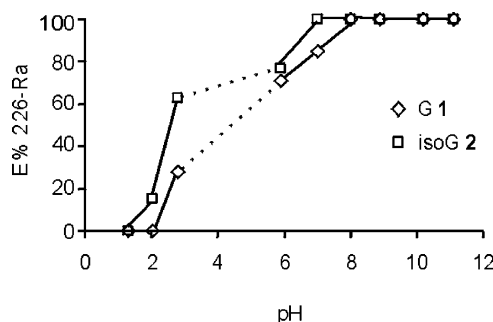


Figure 4. Influence of the pH on the $^{226}\text{Ra}^{2+}$ extraction of G 1–picrate and isoG 2 assemblies.²⁶

attributed to its lower $^{226}\text{Ra}^{2+}$ selectivity in the presence of these cations (for details see Supporting Information).

Extraction of $^{226}\text{Ra}^{2+}$ by G 1–picrate and isoG 2 assemblies occurs even in the presence of a 0.35×10^6 -fold excess of monovalent alkali cations. Additionally, $^{226}\text{Ra}^{2+}$ “precipitation” is significantly prevented by the presence of both G 1 and isoG 2. Clearly, the noncovalent assemblies formed by G 1 and isoG 2 are much more favorable at binding divalent $^{226}\text{Ra}^{2+}$ cations than monovalent alkali cations (Scheme 2).

Determination of the Effective pH Range. The pH profiles for $^{226}\text{Ra}^{2+}$ extraction by G 1–picrate and isoG 2 assemblies, obtained under noncompetitive conditions, indicate that both these nucleosides are effective $^{226}\text{Ra}^{2+}$ extractants between pH 3 and pH 11 (Figure 4).

Between pH 2 and pH 8 the extraction efficiency shows an upward trend for both the G 1–picrate and the isoG 2 assemblies, and above pH 8 the $^{226}\text{Ra}^{2+}$ extraction becomes quantitative. This significantly improves the effective pH region compared to that reported by Chen et al. for self-neutralizing systems (pH 6–11) viz. *p*-tert-butylcalix[4]arene-crown-6-dicarboxylic acid, *p*-tert-butylcalix[4]arene-crown-6-dihydroxamic acid, a 17-crown-5 ether with one pendant carboxylic acid group, and an acyclic polyether with two pendant carboxylic acid groups.¹¹ To verify the results obtained with the low $^{226}\text{Ra}^{2+}$ concentrations used ($[\text{I}]/[^{226}\text{Ra}^{2+}] = 3.5 \times 10^3$), extraction experiments were performed using a 4×10^2 excess of Ba^{2+} nitrate and 2 equiv of LiPic in the case of G 1. These experiments were monitored by ^1H NMR spectroscopy for the formation of the corresponding G 1–picrate and isoG 2 assemblies. The hexadecameric assembly of G 1, $[\text{G } 1]_{16} \cdot 2\text{Ba}^{2+} \cdot 4\text{Pic}^-$, was shown to be stable between pH 2 and 11. Below

pH 2, the picrate ($pK_a = 0.38$ in water)²⁷ peak and signals for $[G\ 1]_{16} \cdot 2Ba^{2+} \cdot 4Pic^-$ broaden and NMR signals for “free” **G 1** are observed. Above pH 11, NMR signals for the G-quadruplex $[G\ 1]_{16} \cdot 2Ba^{2+} \cdot 4Pic^-$ could no longer be observed.²⁸ Characteristic NMR signals for the isoG **2** decamer, $[isoG\ 2]_{10} \cdot Ba^{2+}$, were also observed between pH 3 and 11. Below pH 3, an additional NH signal appeared and only partial complex formation was observed, while, above pH 11, the characteristic NH1 signals of the decamer $[isoG\ 2]_{10} \cdot Ba^{2+}$ were no longer present.²⁹ Assembly formation is clearly influenced by the presence of charges on the nucleoside monomers, as generated by protonation or deprotonation of the NH groups. Nevertheless, the effective pH range covers a broad region, making assemblies of **G 1** and isoG **2** widely applicable ionophores.

Conclusions

The noncovalent assemblies formed by **G 1** and isoG **2** show high $^{226}Ra^{2+}$ selectivities in the presence of divalent alkaline earth cations. Where in the case of **G 1** the presence of a lipophilic anion is required before giving a high $^{226}Ra^{2+}$ selectivity in the case of Mg^{2+} and Ca^{2+} , isoG **2** gives high selectivities in the presence of Mg^{2+} , Ca^{2+} , Sr^{2+} , and Ba^{2+} , without any additional additives.³⁰ Furthermore, a remarkable $^{226}Ra^{2+}$ preference in the presence of monovalent alkali cations, “precipitation preventing/dissolving” characteristics, and a broad effective pH range were observed for both **G 1** and isoG **2**. The ability to quantitatively and selectively extract a highly toxic radioisotope from a solution containing a million-fold excess of other cations shows the power and potential of using molecular self-assembly to construct highly selective receptors.

Experimental Section

Materials. The preparation of **G 1**¹⁷ and isoG **2**³¹ was according to literature procedures. The acids (concentrated HCl and HNO₃) and CH₂-Cl₂ were of p.a. grade and used as received. The nitrate salts of K⁺ ($\geq 99.5\%$) and Rb⁺ (p.a.) were purchased from Fluka Chemie, and those of Na⁺ (p.a.), Cs⁺ (99%), Mg^{2+} (p.a.), Ca^{2+} (p.a.), Sr^{2+} (p.a.), and Ba^{2+} (p.a.) were purchased from Acros Organics. $^{133}Ba^{2+}$ stock solutions were purchased from Isotope Products Europe Blaseg GmbH. $^{226}Ra^{2+}$ stock solutions were purchased from AEA Technology QSA GmbH; ^{226}Ra was used due to its long half-life ($t_{1/2} = 1.6 \times 10^3$ y). (**Note: ^{226}Ra has a very high radiotoxicity and should be handled with care and under radionuclear supervision.**)

Solutions. All basic experiments were performed using an aqueous phase with pH 8.9 (tris-HCl buffer) and an organic phase containing

10^{-4} M of ionophore in CH₂Cl₂. The ionophore concentrations of the organic solutions were based on the amount of “free” ionophore needed to complex one alkaline earth cation ($[G\ 1]_8$, $[isoG\ 2]_{10}$). The different nitrate salt concentrations were obtained by diluting stock solutions to the required concentration. From a $10\ \mu g\ Ba^{2+}/mL$ carrier containing stock solution of $^{133}Ba^{2+}$ in 0.1 M HCl, a dilution of 45.18 kBq/g in water was made. From a carrier free stock solution of $^{226}Ra^{2+}$ in 0.5 M HCl, a dilution of 1.2 kBq/g (1.4×10^{-6} M) in 0.1 M HNO₃ was made.

General Extraction Procedures. Equal volumes (1.0 mL) of the organic and aqueous solutions were transferred into a screw cap vial with a volume of 4 mL. The samples were shaken (1500 rpm) at ambient temperatures (22–24 °C) for 1 h to ensure complete settling of the two-phase equilibration. In the case of the **G 1** extraction experiments 2 molar equiv, compared to $[G\ 1]_8$, of LiPic were added to allow for full extraction. After extraction, the solutions were disengaged by centrifugation (1600 rpm for 5 min), and aliquots (0.5 mL) of the organic and aqueous phases were pipetted out. Experiments were performed in duplicate; average values are reported, with an estimated error of 10–15%.

ICP-MS Monitored Extraction Procedures. The solvent of the aliquot taken from the organic phase was evaporated, and the residue dissolved in 0.5 mL of concentrated HNO₃. The cation concentrations were measured on a Perkin-Elmer Sciex Elan 6000 ICP-MS instrument, using a Cross-flow nebulizer. The extraction percentage is defined as 100% times the ratio of cation concentration in the organic phase ($[M_o]$) and the added cation concentration ($[M_{add}]$) (eq 1).³²

$$E\% = 100\%([M_o]/[M_{add}]) \quad (1)$$

Noncompetitive ICP-MS (Table 1). In the noncompetitive extraction experiments the salt concentrations ($M(NO_3)_2$; $M = Mg^{2+}$, Ca^{2+} , Sr^{2+} , and Ba^{2+}) were equal to those of the ionophores (10^{-4} M) and were verified by their mass balances.

^{133}Ba Tracer Experiments (Table 1). In $^{133}Ba^{2+}$ extraction experiments the exact conditions were used as described above for the ICP-MS experiments. But in this case, $10\ \mu L$ of ^{133}Ba tracer (452 Bq) were added. The gamma activity was determined using a NaI scintillation counter. The obtained extraction percentage is defined as 100% times the ratio of $^{133}Ba^{2+}$ activity in the organic phase (A_o) and the total $^{133}Ba^{2+}$ activity ($A_o + A_{aq}$) (eq 2).

$$E\% = 100\%(A_o/(A_o + A_{aq})) \quad (2)$$

$^{226}Ra^{2+}$ Extraction Procedures. In the case of the $^{226}Ra^{2+}$ extraction experiments, to the aqueous phase $20\ \mu L$ of $^{226}Ra^{2+}$ tracer (240 Bq) were added. The gamma activity was determined with a Ge(Li) scintillation counter. The obtained extraction percentage is defined as 100% times the ratio of $^{226}Ra^{2+}$ activity in the organic phase (A_o) and the total $^{226}Ra^{2+}$ activity ($A_o + A_{aq}$) (eq 2).

Noncompetitive $^{226}Ra^{2+}$ Extractions. In the noncompetitive extraction experiments the aqueous phase only consisted of $^{226}Ra^{2+}$ cations in 1 mL of pH 8.9 tris-HCl buffer. To determine the influence of picrate anions on the extraction behavior of the **G 1** and isoG **2** assemblies, additional experiments were performed in which 2 molar equiv of LiPic (2×10^{-4} M) were added to the aqueous phases.

Competitive $^{226}Ra^{2+}$ Extraction Curves (Single Competing Cation; Figures 2 and 3). In the competitive extraction experiments, aqueous phase pH 8.9 (tris-HCl), the ratio of competing $M^q(NO_3)_n$ ($M = Na^+$, K^+ , Rb^+ , Cs^+ , Mg^{2+} , Ca^{2+} , Sr^{2+} , and Ba^{2+}) salt concentrations compared to a fixed ionophore concentration (1 mL; 10^{-4} M) was altered to provide competing cation-concentration-dependent extraction curves.

Precipitation Experiments (Figure 1). Extraction experiments were performed as described above, but in this case the detectable amount

- (25) At concentrations of 10^{-2} M the total detected amount of $^{226}Ra^{2+}$ cations with **G 1** was almost equal to that originally added ($^{226}Ra^{2+}_{add}$), whereas isoG **2** still showed $^{226}Ra^{2+}$ salt precipitation.
- (26) Due to the competitive nature of the available buffers between pH 3 and 6, the $^{226}Ra^{2+}$ extraction percentages could not be accurately determined in this region. Therefore, the results are extrapolated from those obtained at pH 3 and 6.
- (27) Botoshansky, M.; Herbstein, F. H.; Kapon, M. *Acta Crystallogr. B* **1994**, *32*, 191–200.
- (28) Rogstad, K. N.; Jang, Y. H.; Sowers, L. C.; Goddard, W. A. *Chem. Res. Toxicol.* **2003**, *16*, 1455–1462. The loss of the **G 1** complex stability below pH 2 and above pH 11 appears to match the guanosine pK_a values (NH1 = 9.65 and NH7/NH3 = 3.2) determined in water.
- (29) Jang, Y. H.; Goddard, W. A.; Noyes, K. T.; Sowers, S. H.; Chung, D. S. *J. Phys. Chem. B* **2003**, *107*, 344–357. The loss of the isoG **2** complex stability below pH 3 and above pH 11 appears to match the isoguanosine pK_a values (NH1 = 11.1 and NH3 = 3.8) determined in water.
- (30) A direct comparison with known radium ionophores was not made, due to the different testing methods used. In our case the extraction of $^{226}Ra^{2+}$ cations was performed from a large excess of competing cations using a deficiency of ionophore, while in refs 9 and 11 the extractions have been carried out using an excess of ionophore to competing cations.
- (31) Davis, J. T.; Tirumala, S.; Jenssen, J. R.; Radler, E.; Fabris, D. *J. Org. Chem.* **1995**, *60*, 4167–4176.

- (32) The isotope ^{43}Ca was corrected for the doubly charged interference of the isotope ^{88}Sr .

of $^{226}\text{Ra}^{2+}$ tracer was determined. The organic phase contained dichloromethane; no ionophore was present. The $^{226}\text{Ra}^{2+}$ percentage is defined as 100% times the ratio of $^{226}\text{Ra}^{2+}$ detected in the aqueous phase (A_{aq}) and the amount of $^{226}\text{Ra}^{2+}$ added (A_{add}) (eq 3).

$$\text{Ra}\% = 100\% (A_{\text{aq}}/A_{\text{add}}) \quad (3)$$

Extraction vs pH Curves (Figure 4). Experiments were performed using a fixed ionophore (G **1**)₈ or (isoG **2**)₁₀ concentration of 10^{-4} M and a fixed $^{226}\text{Ra}^{2+}$ concentration (2.9×10^{-8} M). The pH values were set using different buffer solutions: pH 1–3, glycerol–LiCl–HCl (G **1**) and HCl (isoG **2**);³³ pH 6–7, imidazol–HCl; pH 8–10, tris–HCl; and pH 10–13, tris-(CH₃)₃NOH.

¹H NMR Monitored Extraction Experiments. Using the same buffer solutions as mentioned above, solid-phase extraction experiments of Ba(NO₃)₂ (0.1 g; 3.8×10^{-4} mol) were performed with a 1 mL buffer, containing aqueous phase, and a 1.0 mL organic phase, containing 10^{-3} M of ionophore.

(33) Below pH 3, G **1** seemed to have its $^{226}\text{Ra}^{2+}$ extraction interfered by HCl, whereas isoG **2** had its $^{226}\text{Ra}^{2+}$ extraction interfered by glycerol–HCl–LiCl.

Acknowledgment. This research is supported by the Technology Foundation STW, applied science division of NWO and the technology program of the Ministry of Economic Affairs and by the U.S. Department of Energy (JD). We gratefully acknowledge the Fuels, Actinides and Isotopes (FAI) department at the Nuclear Research & Consultancy Group (NRG) in The Netherlands for providing the radionuclear facilities and Mw. T. Tomasberger for her support. We thank C. J. H. Miermans from the Information and Measurement Technology Laboratory for Inorganic Analysis (IMLA) department at the Institute for inland Water Management and Wastewater Treatment (RIZA) for performing the ICP-MS measurements.

Supporting Information Available: Overall $^{226}\text{Ra}^{2+}$ percentages present in solutions with varying concentrations of alkali-(ne earth) cations, after extraction with G **1** and isoG **2**, are given. This material is available free of charge via the Internet at <http://pubs.acs.org>.

JA0455650